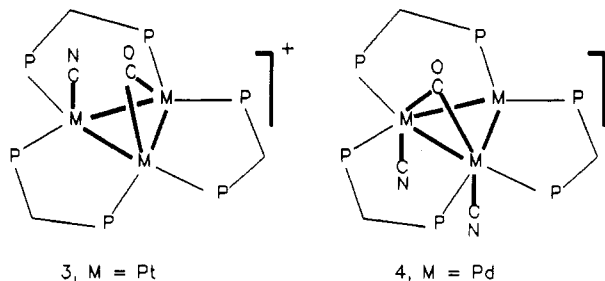


2 shows the simpler mechanism with a μ_3 -CN intermediate.

While the complexes 2 have the same structure for M = Pd and Pt, intermediates in their formation from 1 and CN^- at low temperature were different and are characterized as $[\text{Pt}_3(\text{CN})(\mu_2\text{-CO})(\mu\text{-dppm})_3]^+$ (3) and $[\text{Pd}_3$ -



$(\text{CN})_2(\mu_2\text{-CO})(\mu\text{-dppm})_3$] (4), respectively, by their low-temperature NMR spectra.⁶ These complexes were not fluxional at -40°C , and for example, 3 gave a ^{13}C resonance for the cyanide ligand which appeared as a 1:4:1 triplet due

(6) NMR for 3 in CD_2Cl_2 at -40°C : $\delta(^{31}\text{P}) = -25.9$ [m, $^3J(\text{P}^a\text{P}^c) = 212$, $^2J(\text{P}^a\text{P}^b) = 19$, $^1J(\text{PtP}^a) = 3380$ Hz, P^a], -43.7 [m, $^3J(\text{P}^a\text{P}^c) = 212$, $^2J(\text{P}^b\text{P}^c) = 13$, $^1J(\text{PtP}^c) = 2240$ Hz, P^c], -61.1 [t, $^2J(\text{P}^b\text{P}^c) = 12.8$, $^1J(\text{PtP}^b) = 2920$, $^2J(\text{PtP}^b) = 412$, $^3J(\text{P}^b\text{P}^b) = 228$ Hz, P^b]; $\delta(^{13}\text{C}) = 232.3$ [d, $^2J(\text{C}^a\text{C}^b) = 20$, $^1J(\text{PtC}^a) = 860$, $^2J(\text{PtC}^a) = 130$ Hz, $\mu\text{-C}^a\text{O}$], 131.7 [d, $^2J(\text{C}^a\text{C}^b) = 20$, $^1J(\text{PtC}^b) = 984$ Hz, C^bN]. NMR for 4 in CD_2Cl_2 at -40°C : $\delta(^{31}\text{P}) = 13.8$ [t, $^2J(\text{P}^a\text{P}^c) = 26.2$, $^2J(\text{P}^a\text{C}^a) = 29$ Hz, P^a], 11.8 [t, $^2J(\text{P}^b\text{P}^c) = 49.8$ Hz, P^b], -0.6 [t, $^2J(\text{P}^b\text{P}^c) = 50$, $^2J(\text{P}^a\text{P}^c) = 26$ Hz, P^c]; $\delta(^{13}\text{C}) = 235.3$ [m, $^2J(\text{P}^a\text{C}^a) = 29$, $\mu\text{-C}^a\text{O}$], 135.5 [td, $^2J(\text{CP}) = 17$, $^2J(\text{C}^b\text{C}^c) = 42$ Hz, C^bN], 131.7 [td, $^2J(\text{CP}) = 12$, $^2J(\text{C}^b\text{C}^c) = 42$ Hz, C^cN].

to $^1J(^{195}\text{PtC}) = 984$ Hz, as expected for a terminal cyanide.^{2b,c}

The above data clearly establish that, in these model complexes, cyanide has a lower tendency than the iso-electronic carbonyl to act as a μ_2 -C- or μ_3 -C-bonded ligand (or a higher tendency to act as a terminal ligand) on the Pd_3 or Pt_3 triangle. No evidence for the bonding mode D, thought to be present on the $\text{Pd}(111)$ or $\text{Pt}(111)$ surface,¹ was found; this bonding mode, in which cyanide acts as a 4-electron ligand, is theoretically possible since the clusters 2 are still coordinatively unsaturated (44e clusters). Instead, the terminal cyanide bonding can be considered to model cyanide adsorbed on $\text{Ni}(111)$ and several other metal surfaces.¹ The very easy mobility of terminal cyanide between metal centers, established here for the first time, suggests that a similar surface mobility can be expected and indicates that there is only a small energy difference between terminal and bridging cyanide bonding modes.

Acknowledgment. We thank the NSERC (Canada), NATO, and the SERC (U.K.) for financial support and the Kenyan High Commission for a studentship (to B.N.M.).

Supplementary Material Available: Text giving crystallographic details and tables of hydrogen atom parameters, anisotropic displacement parameters, and bond lengths and angles (8 pages). Ordering information is given on any current masthead page.

OM920412J

Kinetics and Mechanism of Photochemical Substitution Reactions of $\text{Cp}_2\text{Fe}_2(\text{CO})_4$

Shulin Zhang and Theodore L. Brown*

School of Chemical Sciences, University of Illinois at Urbana-Champaign, Urbana, Illinois 61801

Received June 5, 1992

The photochemical reactions of $\text{Cp}_2\text{Fe}_2(\text{CO})_4$ with various nucleophiles (L) in solution have been studied employing flash photolysis methods. The products of reactions were identified using IR spectroscopy, and formation of monosubstituted products $\text{Cp}_2\text{Fe}_2(\text{CO})_3\text{L}$ were observed. It appears that the L = $\text{P}(\text{OMe})_3$, $\text{P}(\text{OEt})_3$, $\text{P}(\text{O}-i\text{-Pr})_3$, $\text{P}(\text{OBu})_3$, $\text{P}(\text{OPh})_3$, PPh_3 , $\text{P}(i\text{-Pr})_3$, PCy_3 , $\text{PPh}_2(\text{C}_6\text{F}_5)$, $\text{PPh}(\text{C}_6\text{F}_5)_2$, and CH_3CN derivatives occur as a mixture of cis and trans isomers in solution, whereas the PEt_3 , PPr_3 , PBu_3 , $\text{P}(t\text{-Bu})_3$, $\text{P}(o\text{-tolyl})_3$, $\text{P}(\text{mesityl})_3$, and 1-hexene derivatives are present as predominantly one isomer. The derivatives of L = $\text{P}(\text{mesityl})_3$, $\text{PPh}_2(\text{C}_6\text{F}_5)$, $\text{PPh}(\text{C}_6\text{F}_5)_2$, $\text{P}(\text{C}_6\text{F}_5)_3$, and 1-hexene are not stable at room temperature. For L = $\text{P}(\text{OMe})_3$, both $\text{Cp}_2\text{Fe}_2(\text{CO})_3\text{P}(\text{OMe})_3$ and the disubstituted product $[\text{CpFe}(\text{CO})\text{P}(\text{OMe})_3]_2$ were observed at room temperature after a single flash photolysis of $\text{Cp}_2\text{Fe}_2(\text{CO})_4$ with $\text{P}(\text{OMe})_3$. An intermediate, possibly $\text{Cp}_2\text{Fe}_2(\text{CO})(\mu\text{-CO})(\eta^2\text{-HC}\equiv\text{CBu})$, was observed as a precursor to the alkyne insertion product, $\text{Cp}_2\text{Fe}_2(\text{CO})(\mu\text{-CO})(\mu\text{-}\sigma\text{-}\eta^3\text{-HC}\equiv\text{CBuCO})$, in the flash photolysis of $\text{Cp}_2\text{Fe}_2(\text{CO})_4$ with 1-hexyne. The kinetics and mechanism of reactions of $\text{Cp}_2\text{Fe}_2(\mu\text{-CO})_3$ with various ligands were investigated via studies of reaction rate law, determination of activation parameters, and analysis of kinetics data in terms of linear-free-energy relationships. Two possible reaction pathways, i.e., an associative bimolecular pathway and a nonassociative pathway involving an intramolecular bridge-cleavage step, are discussed. A consistent rate enhancement effect by an unsubstituted phenyl ring or oxygen atom in the ligand is evident in the data.

Introduction

The photochemical reactions of $\text{Cp}_2\text{Fe}_2(\text{CO})_4$ ($\text{Cp}(\text{CO})\text{Fe}(\mu\text{-CO})_2\text{Fe}(\text{CO})\text{Cp}$) continue to attract attention.¹⁻⁷ It

has been established that photolysis of $\text{Cp}_2\text{Fe}_2(\text{CO})_4$ generates 17-electron radicals, $\text{Cp}(\text{CO})_2\text{Fe}^*$, via homolysis of

(1) (a) Geoffroy, G. L.; Wrighton, M. S. *Organometallic Photochemistry*; Academic Press: New York, 1979. (b) Abrahamson, H. B.; Palazzotto, M. C.; Reichel, C. L.; Wrighton, M. S. *J. Am. Chem. Soc.* 1979, 101, 4123. (c) Hepp, A. F.; Blaha, J. P.; Lewis, C.; Wrighton, M. S. *Organometallics* 1984, 3, 174.

(2) (a) Caspar, J. V.; Meyer, T. J. *J. Am. Chem. Soc.* 1980, 102, 7794. (b) Meyer, T. J.; Caspar, J. V. *Chem. Rev.* 1985, 85, 187.

(3) (a) Tyler, D. R.; Schmidt, M. A.; Gray, H. B. *J. Am. Chem. Soc.* 1979, 101, 2753. (b) Tyler, D. R.; Schmidt, M. A.; Gray, H. B. *J. Am. Chem. Soc.* 1983, 105, 6018. (c) Goldman, A. S.; Tyler, D. R. *Inorg. Chem.* 1987, 26, 253. (d) Castellani, M. P.; Tyler, D. R. *Organometallics* 1989, 8, 2113. (e) Tyler, D. R. In *Organometallic Radical Processes*; Trogler, W. C., Ed.; Elsevier: Amsterdam, 1990; p 338.

the Fe-Fe bond, and a triply-carbonyl-bridged species, $\text{Cp}_2\text{Fe}_2(\mu\text{-CO})_3$, via cleavage of an Fe-CO bond.^{1a,2} Recently, a second CO-bridging species, $\text{Cp}_2\text{Fe}_2(\mu\text{-CO})_2(\mu\text{-}\eta^1, \eta^2\text{-CO})$, resulting from CO loss, has been identified as a minor photoproduct,^{8a,9} and the role of radicals in the formation of $\text{Cp}_2\text{Fe}_2(\mu\text{-CO})_3$ has been described.⁹

$\text{Cp}_2\text{Fe}_2(\text{CO})_4$ undergoes photochemical substitution of carbonyl groups by nucleophiles.¹⁰ An unstable species, $\text{Cp}(\text{CO})_2\text{Fe}-\text{C}(\text{O})-\text{Fe}(\text{CO})\text{Cp}$, in which a single CO bridges the Fe atoms and there is no direct Fe-Fe bond, was proposed as an intermediate in the substitution reaction with $\text{P}(\text{O}-i\text{-Pr})_3$.^{3a,b} The 17-electron radical, $\text{Cp}(\text{CO})_2\text{Fe}^\bullet$, was also proposed to be an intermediate in the substitution reactions.^{1b} Disubstituted products, where observed, typically arise via substitution of the radical, followed by recombination. However evidence from flash photolysis experiments of $\text{Cp}_2\text{Fe}_2(\text{CO})_4$ indicates that the CO-loss intermediate, $\text{Cp}_2\text{Fe}_2(\text{CO})_3$, is responsible for formation of monosubstituted product, $\text{Cp}_2\text{Fe}_2(\text{CO})_3\text{L}$.^{2a}

Flash photolysis studies using UV-vis or IR detection have demonstrated that $\text{Cp}(\text{CO})_2\text{Fe}^\bullet$ radicals recombine rapidly ($k \approx 3 \times 10^9 \text{ M}^{-1} \text{ s}^{-1}$ in cyclohexane at 22 °C) to re-form $\text{Cp}_2\text{Fe}_2(\text{CO})_4$.^{2a} They also undergo rapid substitution by $\text{P}(\text{OMe})_3$ to form $\text{Cp}(\text{CO})\text{FeP}(\text{OMe})_3$ ($k \approx (8.9 \pm 2.0) \times 10^8 \text{ M}^{-1} \text{ s}^{-1}$ in *n*-heptane at 25 °C).^{4e} However, $\text{Cp}(\text{CO})_2\text{Fe}^\bullet$ appears to react more slowly with PPh_3 , PBU_3 , or CH_3CN .^{4e} The reaction kinetics of $\text{Cp}_2\text{Fe}_2(\mu\text{-CO})_3$ with a few nucleophiles to generate the monosubstituted product, $\text{Cp}_2\text{Fe}_2(\text{CO})_3\text{L}$, also have been studied using flash photolysis methods.^{2a,4c,7b} The reaction is first order each in $\text{Cp}_2\text{Fe}_2(\mu\text{-CO})_3$ and L. The activation parameters (ΔH^\ddagger , ΔS^\ddagger) measured for these reactions are consistent with an associative bimolecular pathway.^{4c,7b} It has been proposed that reaction of an analogous semibridging photochemical intermediate, $\text{L}(\text{CO})_3\text{Mn}(\mu\text{-}\eta^1, \eta^2\text{-CO})\text{Mn}(\text{CO})_3\text{L}$ (L = phosphine), with HSnBu_3 involves an intramolecular bridge-cleavage step which is kinetically important.¹¹

In an effort to understand further the photochemical behavior of $\text{Cp}_2\text{Fe}_2(\text{CO})_4$, we have studied its reactions with various nucleophiles, employing flash photolysis with UV-vis and IR detection, both in solution at room temperature and in low-temperature organic glasses.^{8a,9} In this contribution, we report extensive studies on the kinetics and mechanism of substitution reactions of $\text{Cp}_2\text{Fe}_2(\mu\text{-CO})_3$ with nucleophiles in solutions at room temperature.

Experimental Section

All experiments were carried out under an atmosphere of purified argon employing Schlenk techniques, or were performed in a glovebox. Infrared spectra were recorded on a Perkin-Elmer 1710 FTIR spectrometer (2-cm⁻¹ resolution) using 1.0 mm KCl solution cells with Teflon stoppers. $\text{Cp}_2\text{Fe}_2(\text{CO})_4$ (Strem Chemicals) was used without further purification. Purification procedures for *n*-hexane (Burdick and Jackson) and carbon monoxide (Matheson Gas Products, Matheson purity grade, 99.99+%) have been described previously.¹²

PPh_3 (Aldrich) and PCy_3 (Cy = C₆H₁₁, cyclohexyl; Alfa Products) were recrystallized from EtOH and dried under vacuum. 1-Hexene (Aldrich) was distilled over anhydrous MgSO₄. $\text{P}(\text{OPh})_3$ (Aldrich) was distilled over anhydrous MgSO₄ under reduced pressure (160 °C, ~0.1 mmHg). PBU_3 (Aldrich) was distilled over LiAlH₄ (140 °C, ~30 mmHg). $\text{P}(\text{O}-i\text{-Pr})_3$ (Aldrich), $\text{P}(\text{OMe})_3$ (Aldrich), and CH_3CN (Mallinckrodt) were all distilled over CaH₂. $\text{P}(i\text{-Pr})_3$ and $\text{P}(t\text{-Bu})_3$, both from Strem Chemicals in sealed ampule tubes, were opened in an Ar atmosphere glovebox and used as received. $\text{P}(\text{C}_6\text{F}_5)_3$, $\text{PPh}_2(\text{C}_6\text{F}_5)_2$, $\text{PPh}(\text{C}_6\text{F}_5)_2$, $\text{P}(o\text{-tolyl})_3$, and 1-hexyne from Aldrich and $\text{P}(\text{mesityl})_3$ from Alfa were used as received.

The flash photolysis experiments were carried out as described previously;¹¹⁻¹³ we employ a conventional flash photolysis apparatus, consisting of two linear high-pressure xenon-flash tubes. The xenon source provides broad UV-vis irradiation; the sample tubes were constructed from Pyrex glass. The monitoring wavelength of 510 nm (λ_{max} for $\text{Cp}_2\text{Fe}_2(\mu\text{-CO})_3$) and pseudo-first-order reaction conditions were employed in the kinetics measurements. For reactions of $\text{Cp}_2\text{Fe}_2(\text{CO})_4$ with phosphorus ligands, precautions were taken to avoid the unwanted thermal reaction or photoreaction induced by room lights. Thus, the ligand and $\text{Cp}_2\text{Fe}_2(\text{CO})_4$ were first loaded into separate branches of the cell used for flash photolysis, and the solutions were mixed in the dark immediately before taking the flash photolysis measurement. The rate constants were calculated based on the transient signal from the first flash. Flash photolysis of $\text{Cp}_2\text{Fe}_2(\text{CO})_4$ and CH_3CN was also performed using a laser flash photolysis system with 308-nm excimer (XeCl) laser excitation (30 ns pulse width) and a Hewlett-Packard HP54111D data acquisition system.

To obtain the IR spectra of a solution after flash photolysis, the IR cell was placed between the xenon-flash tubes and then immediately moved to the IR spectrometer following the flash. Typically, four scans were collected for each spectrum with 2-cm⁻¹ resolution, which takes about 1 min.

Results and Discussion

Reaction Products. The products of photochemical reaction between $\text{Cp}_2\text{Fe}_2(\text{CO})_4$ and various nucleophiles were identified using IR spectroscopy. A hexane solution containing $\text{Cp}_2\text{Fe}_2(\text{CO})_4$ and the ligand (0.005–0.1 M) is loaded into a 1.0-mm KCl cell with Teflon stoppers under Ar. After exposing to a single flash (pulse width $\approx 100 \mu\text{s}$), the cell is moved to the IR spectrometer within 20–40 s. A series of IR spectra were then taken to monitor changes occurring from 1 min to several hours following the flash.

(A) Reactions with Phosphorus Ligands. Thermal or photochemical reactions of many phosphines and phosphites with $\text{Cp}_2\text{Fe}_2(\text{CO})_4$ have been shown to afford the monosubstituted product $\text{Cp}_2\text{Fe}_2(\text{CO})_3\text{L}$. By spectral comparison with authentic samples,^{10b} the observed products are identified as in Table I. The derivatives of $\text{P}(i\text{-Pr})_3$, PCy_3 , $\text{P}(t\text{-Bu})_3$, $\text{P}(\text{C}_6\text{F}_5)_3$, $\text{PPh}_2(\text{C}_6\text{F}_5)_2$, $\text{PPh}(\text{C}_6\text{F}_5)_2$, $\text{P}(o\text{-tolyl})_3$, and $\text{P}(\text{mesityl})_3$ represent new compounds. On the basis of the number of observed terminal CO stretching modes in the IR spectra, Haines and Du Preez have indicated that the phosphine- or phosphite-substituted derivatives exist as *cis* and *trans* isomers in solution,^{10b} as

(12) Zhang, S.; Dobson, G. R.; Brown, T. L. *J. Am. Chem. Soc.* 1991, 113, 6908.

(13) Herrick, R. S.; Herrinton, T. R.; Walker, H. W.; Brown, T. L. *Organometallics* 1985, 4, 42.

(4) (a) Moore, B. D.; Simpson, M. B.; Poliakoff, M.; Turner, J. J. *J. Chem. Soc., Chem. Commun.* 1984, 972. (b) Moore, B. D.; Simpson, M. B.; Poliakoff, M.; Turner, J. J. *J. Phys. Chem.* 1985, 89, 850. (c) Dixon, A. J.; Healy, M. A.; Poliakoff, M.; Turner, J. J. *J. Chem. Soc., Chem. Commun.* 1986, 994. (d) Moore, B. D.; Poliakoff, M.; Turner, J. J. *J. Am. Chem. Soc.* 1986, 108, 1819. (e) Dixon, A. J.; Gravelle, S. J.; van de Burgt, L. J.; Poliakoff, M.; Turner, J. J.; Weitz, E. *J. Chem. Soc., Chem. Commun.* 1987, 1023. (f) Dixon, A. J.; George, M. W.; Hughes, C.; Poliakoff, M.; Turner, J. J. *J. Am. Chem. Soc.* 1992, 114, 1719.

(5) (a) Hooker, R. H.; Mahmoud, K. A.; Rest, A. J. *J. Chem. Soc., Chem. Commun.* 1983, 1022. (b) Hooker, R. H.; Rest, A. J. *J. Chem. Soc., Dalton Trans.* 1990, 1221. (c) Bloyce, P. E.; Campen, A. K.; Hooker, R. H.; Rest, A. J.; Thomas, N. R.; Bitterwolf, T. E.; Shade, J. E. *J. Chem. Soc., Dalton Trans.* 1990, 2833.

(6) (a) Moore, J. N.; Hansen, P. A.; Hochstrasser, R. M. *J. Am. Chem. Soc.* 1989, 111, 4563. (b) Anfirud, P. A.; Han, C.-H.; Lian, T.; Hochstrasser, R. M. *J. Phys. Chem.* 1991, 95, 574.

(7) (a) Bursten, B. E.; Cayton, R. H. *J. Am. Chem. Soc.* 1986, 108, 8241. (b) Bursten, B. E.; Mckee, S. D.; Platz, M. S. *J. Am. Chem. Soc.* 1989, 111, 3428.

(8) (a) Zhang, S.; Brown, T. L. *J. Am. Chem. Soc.* 1992, 114, 2723. (b) Zhang, S.; Brown, T. L. *Organometallics* 1992, 11, 2122.

(9) Zhang, S.; Brown, T. L. *J. Am. Chem. Soc.*, in press.

(10) (a) Mills, O. S. *Acta Crystallogr.* 1958, 11, 620. (b) Haines, R. J.; Du Preez, A. L. *Inorg. Chem.* 1969, 8, 1459. (c) Giannotti, C.; Merle, G. *J. Organomet. Chem.* 1976, 105, 97. (d) Labinger, J. A.; Madhavan, S. *J. Organomet. Chem.* 1977, 134, 381.

(11) (a) Sullivan, R. J.; Brown, T. L. *J. Am. Chem. Soc.* 1991, 113, 9155. (b) Sullivan, R. J.; Brown, T. L. *J. Am. Chem. Soc.* 1991, 113, 9162.

Table I. IR Data for Relevant Compounds in Hexane

compound	ν_{CO} , cm^{-1} (rel intensity) ^a
$\text{Cp}_2\text{Fe}_2(\text{CO})_4$	2006 (1.0), 1961 (2.1), 1794 (2.1)
$\text{Cp}_2\text{Fe}_2(\text{CO})_3\text{PPh}_3$	1962 (1.4), 1938 (1.0), 1742 (2.7)
$\text{Cp}_2\text{Fe}_2(\text{CO})_3\text{PBu}_3$	1934 (1.0), 1747 (1.8)
$\text{Cp}_2\text{Fe}_2(\text{CO})_3\text{P}(i\text{-Pr})_3$	1953 (1.0), 1935 (2.6), 1745 (4.5)
$\text{Cp}_2\text{Fe}_2(\text{CO})_3\text{P}(\text{OMe})_3$	1966 (2.8), 1947 (1.0), 1753 (4.0)
$[\text{CpFe}(\text{CO})\text{P}(\text{OMe})_3]_2$	1716
$\text{Cp}_2\text{Fe}_2(\text{CO})_3\text{P}(O\text{-}i\text{-Pr})_3$	1963 (3.8), 1941 (1.0), 1755 (5.8)
$\text{Cp}_2\text{Fe}_2(\text{CO})_3\text{P}(\text{OPh})_3$	1973 (1.5), 1950 (1.0), 1762 (2.4)
$\text{Cp}_2\text{Fe}_2(\text{CO})_3\text{PCy}_3$	1951 (1.5), 1929 (1.0), 1746 (1.7)
$\text{Cp}_2\text{Fe}_2(\text{CO})_3\text{P}(t\text{-Bu})_3$	1946 (1.0), 1754 (1.0)
$\text{Cp}_2\text{Fe}_2(\text{CO})_3\text{P}(o\text{-tolyl})_3$	1950 (1.0), 1751 (1.0)
$\text{Cp}_2\text{Fe}_2(\text{CO})_3\text{P}(\text{mesityl})_3$ ^b	1951 (1.0), 1749 (1.0)
$\text{Cp}_2\text{Fe}_2(\text{CO})_3\text{PPh}_2(\text{C}_6\text{F}_5)$ ^c	1970 (1.0), 1949 (1.8), 1749 (2.6)
$\text{Cp}_2\text{Fe}_2(\text{CO})_3\text{PPh}(\text{C}_6\text{F}_5)_2$ ^d	1972 (1.2), 1955 (1.0), 1757 (2.8)
$\text{Cp}_2\text{Fe}_2(\text{CO})_3(\text{C}_6\text{F}_5)_3$ ^e	1958 (1.1), 1765 (1.0)
$\text{Cp}_2\text{Fe}_2(\text{CO})_3(\text{CH}_3\text{CN})$ ^f	1945 (2.0), 1765 (3.0), 1755 (1.0)
$\text{Cp}_2\text{Fe}_2(\text{CO})_3(\eta^2\text{-H}_2\text{C}=\text{CHBu})$ ^g	1962, 1772
$\text{Cp}_2\text{Fe}_2(\text{CO})(\mu\text{-CO})_2(\eta^2\text{-HC}\equiv\text{CBu})$	1968 (1.7), 1955 (6.2), 1820 (5.2), 1770 (1.0)
$\text{Cp}_2\text{Fe}_2(\text{CO})(\mu\text{-CO})(\mu\text{-}\sigma\text{-}\eta^3\text{-HC}\equiv\text{CBuCO})$	1988 (9.9), 1969 (1.0), 1818 (4.1), 1775 (1.1)

^aRelative intensity calculated based on the absorbance at the band maxima. ^bNot stable, $t_{1/2} \approx 3$ min. ^cNot stable, $t_{1/2} \approx 3$ min. ^dNot stable, $t_{1/2} \approx 1$ min. ^eIn 3MP at -70°C , not observed at room temperature. ^fWith 0.085 M CH_3CN in hexane. ^gNot stable, $t_{1/2} \approx 1$ min.

with $\text{Cp}_2\text{Fe}_2(\text{CO})_4$. It appears that the $\text{L} = \text{P}(\text{OMe})_3$, $\text{P}(\text{OEt})_3$, $\text{P}(O\text{-}i\text{-Pr})_3$, $\text{P}(\text{OBu})_3$, $\text{P}(\text{OPh})_3$, PPh_3 , $\text{P}(i\text{-Pr})_3$, PCy_3 , $\text{PPh}_2(\text{C}_6\text{F}_5)$, and $\text{PPh}(\text{C}_6\text{F}_5)_2$ derivatives occur as a mixture of cis and trans isomers in solution, whereas the PEt_3 , PPr_3 , PBu_3 , $\text{P}(t\text{-Bu})_3$, $\text{P}(o\text{-tolyl})_3$, and $\text{P}(\text{mesityl})_3$ derivatives are present as predominantly one isomer. The appearance of a single peak in the bridging CO stretching region of the IR spectra of $\text{Cp}_2\text{Fe}_2(\text{CO})_3\text{L}$ ($\text{L} = \text{CO}$, phosphine or phosphite) has been attributed to the accidental degeneracy of the symmetric and asymmetric modes of either isomer or the negligible intensity of the symmetric mode. In addition, the bridging CO frequency of the trans isomer must be approximately equal to that of the cis isomer for a given ligand, to account for the presence of only a single band in the bridging region when both cis and trans isomers are present.^{10b}

The IR spectra after flash photolysis of $\text{Cp}_2\text{Fe}_2(\text{CO})_4$ with $\text{P}(o\text{-tolyl})_3$ are relatively complex. Besides the IR bands at 1950 and 1751 cm^{-1} , assignable to $\text{Cp}_2\text{Fe}_2(\text{CO})_3\text{P}(o\text{-tolyl})_3$, other bands are also observed. Similar results are obtained with $\text{P}(\text{mesityl})_3$. Further characterizations of the other products are currently underway. It is noted that $\text{Cp}_2\text{Fe}_2(\text{CO})_3\text{P}(\text{mesityl})_3$, $\text{Cp}_2\text{Fe}_2(\text{CO})_3\text{PPh}_2(\text{C}_6\text{F}_5)$, and $\text{Cp}_2\text{Fe}_2(\text{CO})_3\text{PPh}(\text{C}_6\text{F}_5)_2$ are not stable at room temperature; they disappear rapidly with $t_{1/2} \approx 3, 3,$ and 1 min, respectively.

No net photoreaction product was observed when $\text{P}(\text{C}_6\text{F}_5)_3$ was photolyzed with $\text{Cp}_2\text{Fe}_2(\text{CO})_4$ at room temperature as indicated by the IR spectrum taken 20 s after a flash. At -70°C in 3-methylpentane (3MP), bands observed at 1958 and 1765 cm^{-1} are assignable to the substitution product, $\text{Cp}_2\text{Fe}_2(\text{CO})_3\text{P}(\text{C}_6\text{F}_5)_3$. The product is apparently too unstable to be observed at room temperature.

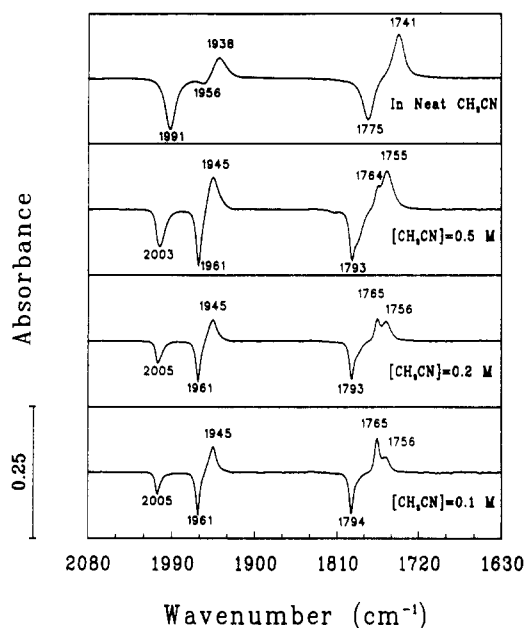


Figure 1. Difference IR spectra following a single flash of $\text{Cp}_2\text{Fe}_2(\text{CO})_4$ in neat CH_3CN or in hexane with CH_3CN present in various concentrations.

The instability of derivatives of $\text{P}(\text{mesityl})_3$, $\text{PPh}_2(\text{C}_6\text{F}_5)$, $\text{PPh}(\text{C}_6\text{F}_5)_2$, and $\text{P}(\text{C}_6\text{F}_5)_3$ can be attributed to the very large steric requirement of $\text{P}(\text{mesityl})_3$ and a combination of large steric requirement and low nucleophilicities for $\text{PPh}_2(\text{C}_6\text{F}_5)$, $\text{PPh}(\text{C}_6\text{F}_5)_2$ and $\text{P}(\text{C}_6\text{F}_5)_3$.

(B) Reactions with CH_3CN . $\text{Cp}_2\text{Fe}_2(\text{CO})_3(\text{CH}_3\text{CN})$ has been previously identified.^{10d} Its IR spectrum shows bands at 1950 and 1725 cm^{-1} in Nujol mull.^{10d} Turner and co-workers observed CO stretching bands at 1945 and 1764 cm^{-1} in cyclohexane.^{4c} We have examined the IR spectral changes, following a single flash, of $\text{Cp}_2\text{Fe}_2(\text{CO})_4$ in neat CH_3CN or in hexane with CH_3CN present in various concentrations (Figure 1). It appears that the reaction product $\text{Cp}_2\text{Fe}_2(\text{CO})_3(\text{CH}_3\text{CN})$ also exists as cis and trans isomers. Interestingly, unlike all other known $\text{Cp}_2\text{Fe}_2(\text{CO})_3\text{L}$ ($\text{L} = \text{CO}$, phosphine, and phosphite) complexes, the two isomers of $\text{Cp}_2\text{Fe}_2(\text{CO})_3(\text{CH}_3\text{CN})$ exhibit two different bridging CO stretching frequencies at 1765 and 1756 cm^{-1} . However, the terminal CO stretching frequencies of the isomers are not resolved (2- cm^{-1} instrumental resolution). The isomer ratio seems to be more sensitive to solvent polarity as compared with $\text{Cp}_2\text{Fe}_2(\text{CO})_4$. It has been shown that for $\text{Cp}_2\text{Fe}_2(\text{CO})_4$, polar solvents favor the cis structure.^{14,15} By analogy and assuming that the $\text{CH}_3\text{CN}\text{-Fe}$ bond dipole does not dominate in determining molecular polarity, bands at 1765 and 1756 cm^{-1} can be attributed to *trans*- $\text{Cp}(\text{CO})\text{Fe}(\mu\text{-CO})_2\text{Fe}(\text{CH}_3\text{CN})$ and *cis*- $\text{Cp}(\text{CO})\text{Fe}(\mu\text{-CO})_2\text{Fe}(\text{CH}_3\text{CN})$, respectively.

(C) Reactions with $\text{P}(\text{OMe})_3$. Continuous photolysis of $\text{Cp}_2\text{Fe}_2(\text{CO})_4$ with $\text{P}(\text{OMe})_3$ has been shown to produce both the monosubstituted $\text{Cp}_2\text{Fe}_2(\text{CO})_3\text{P}(\text{OMe})_3$ and disubstituted $[\text{CpFe}(\text{CO})\text{P}(\text{OMe})_3]_2$ products.^{1b} Tyler et al., however, observed the formation of only $[\text{CpFe}(\text{CO})\text{P}(\text{OMe})_3]_2$, without the intermediacy of $\text{Cp}_2\text{Fe}_2(\text{CO})_3\text{P}(\text{OMe})_3$, in the photochemical reaction ($\lambda > 500$ nm) of $\text{Cp}_2\text{Fe}_2(\text{CO})_4$ with $\text{P}(\text{OMe})_3$.^{3a,b} By employing single-flash

(14) (a) Manning, A. R. *J. Chem. Soc. A* 1968, 1319. (b) McArdle, P. A.; Manning, A. R. *J. Chem. Soc. A* 1969, 1948.

(15) (a) Bullitt, J. G.; Cotton, F. A.; Marks, T. J. *J. Am. Chem. Soc.* 1970, 92, 2155. (b) Gansow, O. A.; Burke, A. R.; Vernon, W. D. *J. Am. Chem. Soc.* 1972, 94, 2550. (c) Gansow, O. A.; Burke, A. R.; Vernon, W. D. *J. Am. Chem. Soc.* 1976, 98, 5817.

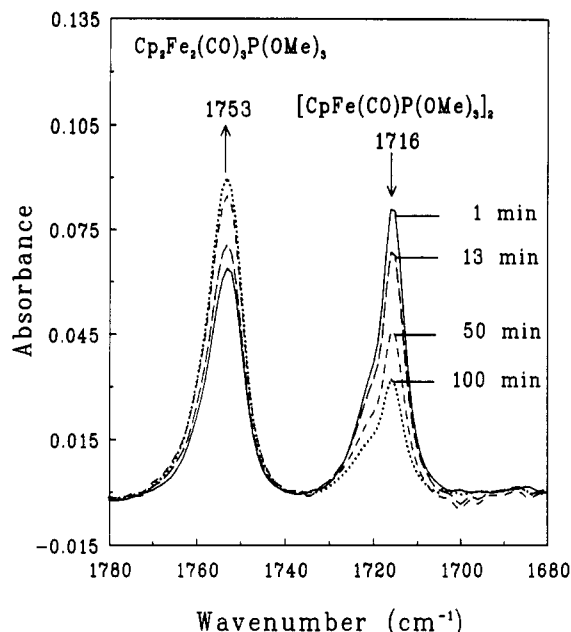
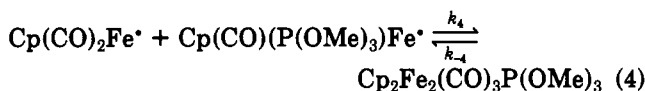
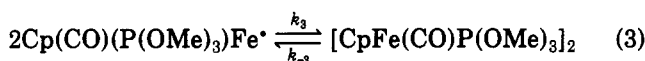
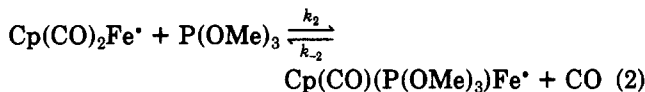
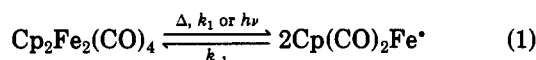


Figure 2. IR spectra of $\text{Cp}_2\text{Fe}_2(\text{CO})_3\text{P}(\text{OMe})_3$ and $[\text{CpFe}(\text{CO})\text{P}(\text{OMe})_3]_2$ observed at various times after a single flash photolysis of $\text{Cp}_2\text{Fe}_2(\text{CO})_4 + \text{P}(\text{OMe})_3$ in hexane solution at room temperature.

photolysis in hexane solution, we observed formation of both $\text{Cp}_2\text{Fe}_2(\text{CO})_3\text{P}(\text{OMe})_3$ and $[\text{CpFe}(\text{CO})\text{P}(\text{OMe})_3]_2$. Figure 2 shows IR bands in the bridging CO stretching region, at 1753 and 1716 cm^{-1} , corresponding to $\text{Cp}_2\text{Fe}_2(\text{CO})_3\text{P}(\text{OMe})_3$ and $[\text{CpFe}(\text{CO})\text{P}(\text{OMe})_3]_2$, respectively. $[\text{CpFe}(\text{CO})\text{P}(\text{OMe})_3]_2$ is not stable under the conditions employed; its disappearance is accompanied by growth in absorption due to $\text{Cp}_2\text{Fe}_2(\text{CO})_3\text{P}(\text{OMe})_3$. The formation and reaction of the disubstituted complex are consistent with a radical pathway (eqs 1–4).



After the flash, $[\text{CpFe}(\text{CO})\text{P}(\text{OMe})_3]_2$ and unreacted $\text{Cp}_2\text{Fe}_2(\text{CO})_4$ can undergo a cross-coupling reaction via Fe–Fe bond homolysis (eq 1, k_1 ; eq 3, k_{-3}) to afford $\text{Cp}_2\text{Fe}_2(\text{CO})_3\text{P}(\text{OMe})_3$. It should be noted that the rate constants (k_1 , k_{-3} , k_{-4}) for thermal homolysis of the Fe–Fe bond are much smaller than those for radical combination (k_{-1} , k_3 , k_4). The immediate formation of $\text{Cp}_2\text{Fe}_2(\text{CO})_3\text{P}(\text{OMe})_3$ upon flash photolysis can be accounted for only in part by reaction 4. It has been demonstrated that the rapid conversion of $\text{Cp}(\text{CO})_2\text{Fe}^{\cdot}$ to $\text{Cp}(\text{CO})(\text{P}(\text{OMe})_3)\text{Fe}^{\cdot}$ favors the disubstituted derivative as the predominant product via the radical mechanism.^{4f} The absence of $\text{Cp}_2\text{Fe}_2(\text{CO})_3\text{P}(\text{OMe})_3$ as a product in the reported experiments using long-wavelength (>500 nm) photolysis^{3a,b} is likely due to a dominant role of the radical mechanism, as opposed to the reaction pathway via the CO-loss intermediate, $\text{Cp}_2\text{Fe}_2(\mu\text{-CO})_3$.

(D) Reactions with 1-Hexene and 1-Hexyne. The photoreaction product between $\text{Cp}_2\text{Fe}_2(\text{CO})_4$ and 1-hexene

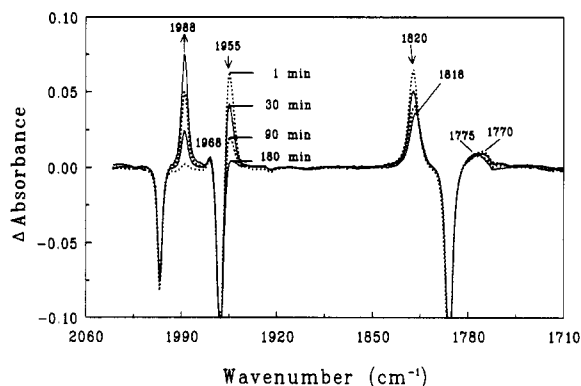
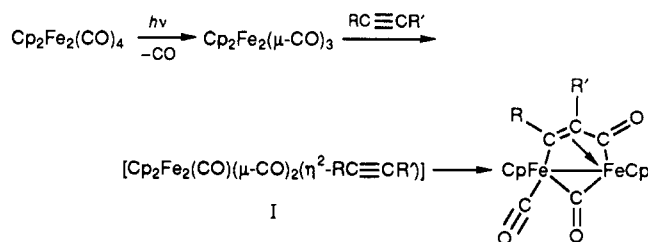


Figure 3. Difference IR spectra observed at various times after a single flash photolysis of $\text{Cp}_2\text{Fe}_2(\text{CO})_4 + 1$ -hexyne in hexane solution at room temperature.

Scheme I



($\text{H}_2\text{C}=\text{CHBu}$), assignable to $\text{Cp}_2\text{Fe}_2(\text{CO})_3(\eta^2\text{-H}_2\text{C}=\text{CHBu})$, is not stable. It was observed in the IR within 20 s after the flash and disappeared over about 60 s. A similar, unstable ethylene complex, $\text{Cp}_2\text{Fe}_2(\text{CO})_3(\eta^2\text{-H}_2\text{C}=\text{CH}_2)$, has been reported.^{16a}

Flash photolysis of $\text{Cp}_2\text{Fe}_2(\text{CO})_4$ in the presence of 1-hexyne ($\text{HC}\equiv\text{CBu}$) afforded the IR spectra shown in Figure 3. The initial product exhibits bands at 1968 (w), 1955 (s), 1820 (s), and 1770 (br, w) cm^{-1} in hexane. These peaks evolved over 3 h into 1988 (vs), 1969 (vw), 1818 (s), and 1775 (w) cm^{-1} . The final spectrum is consistent with the alkyne insertion product, $\text{Cp}_2\text{Fe}_2(\text{CO})(\mu\text{-CO})(\mu\text{-}\sigma\text{:}\eta^3\text{-HC}=\text{CBu})$.^{7b,c} The reactions of alkynes and CO at dinuclear metal centers have been studied by Knox and co-workers.¹⁶ Bursten et al. examined the kinetics of the reaction using laser flash photolysis and proposed a reaction mechanism as shown in Scheme I.^{7b} The proposed intermediate (I) was, however, not spectroscopically identified. The unimolecular transformation of I to the product has been suggested to be faster than formation of I from $\text{Cp}_2\text{Fe}_2(\text{CO})_4$. Our experiments, however, suggest that the intermediate leading to the insertion product is much more stable than previously thought. We have tentatively assigned the initial IR bands after the flash photolysis to $\text{Cp}_2\text{Fe}_2(\text{CO})(\mu\text{-CO})_2(\eta^2\text{-HC}\equiv\text{CBu})$, Table I. However, the observed spectrum could also be consistent with an alternative structure.

Kinetics Studies Using Flash Photolysis. The substitution reaction via a radical pathway, as for $\text{L} = \text{P}(\text{OMe})_3$ (vide supra), is also possible for other ligands. We have studied the flash photolysis of $\text{Cp}_2\text{Fe}_2(\text{CO})_4 + \text{L}$ at

(16) (a) Gracey, B. P.; Knox, S. A. R.; Macpherson, K. A.; Oprea, A. G.; Stobart, S. R. *J. Chem. Soc., Dalton Trans.* 1985, 1935. (b) Dyke, A. F.; Konx, S. A. R.; Naish, P. J.; Taylor, G. E. *J. Chem. Soc., Chem. Commun.* 1980, 409. (c) Dyke, A. F.; Konx, S. A. R.; Naish, P. J.; Taylor, G. E. *J. Chem. Soc., Chem. Commun.* 1980, 803. (d) Dyke, A. F.; Konx, S. A. R.; Naish, P. J.; Taylor, G. E. *J. Chem. Soc., Dalton Trans.* 1982, 1297. (e) Finnimore, S. R.; Konx, S. A. R.; Taylor, G. E. *J. Chem. Soc., Dalton Trans.* 1982, 1783. (f) Casey, C. P.; Miles, W. H.; Fagan, P. J.; Haller, K. J. *Organometallics* 1985, 4, 559.

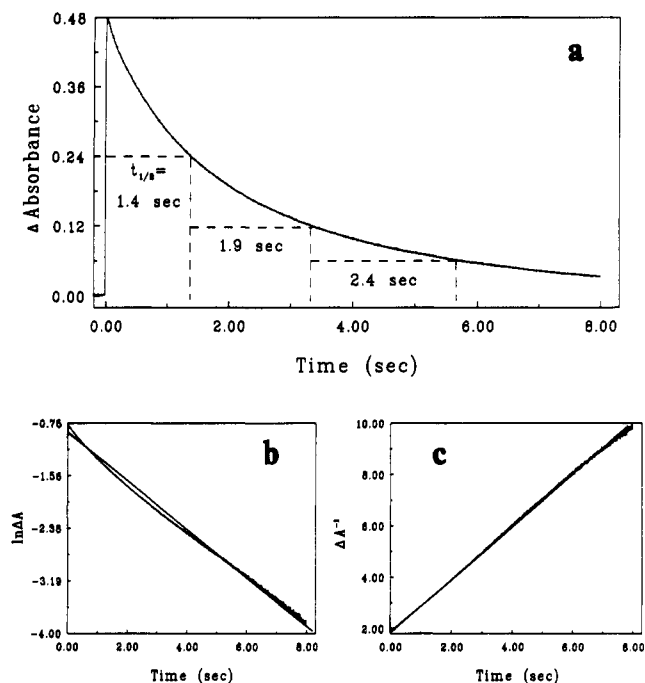
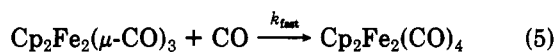


Figure 4. (a) Plot of Δ absorbance vs time at 510 nm following conventional flash photolysis of $\text{Cp}_2\text{Fe}_2(\text{CO})_4$ in hexane under Ar at 25.0 °C. (b) Plot of $\ln(\Delta A)$ vs time ($\Delta A = A_t - A_\infty$). (c) Plot of $(\Delta A)^{-1}$ vs time.

low temperature (−70 °C) with IR detection and observed some species which convert to the substituted products, $\text{Cp}_2\text{Fe}_2(\text{CO})_3\text{L}$, when the solution is warmed to room temperature. We have evidence, to be described elsewhere,⁹ that the transient species are produced via a radical mechanism. In the present paper we focus attention on the kinetics and mechanism of reactions of $\text{Cp}_2\text{Fe}_2(\mu\text{-CO})_3$.

(A) Flash Photolysis under Ar. A plot of Δ absorbance vs time at 510 nm, following conventional flash photolysis of $\text{Cp}_2\text{Fe}_2(\text{CO})_4$ in hexane under Ar, is shown in Figure 4a. This reaction can be attributed to the recombination reaction of $\text{Cp}_2\text{Fe}_2(\mu\text{-CO})_3$ with CO, eq 5. The first half-life of the observed process, $t_{1/2} \approx 1.4$



s, is very close to that observed by Caspar and Meyer ($t_{1/2} \approx 2$ s in cyclohexane).^{2a} They reported that the reaction obeys first-order kinetics and that secondary photolysis occurs due to the probe beam irradiation. Within the time limit of data acquisition (8.2 s), the transient absorbance does not reach a baseline. An optimized computer fit to the data as a first-order process is illustrated in Figure 4b with a plot of $\ln(\Delta A)$ vs time ($\Delta A = A_t - A_\infty$). A fit to the signal as a second-order process, i.e., a plot of $(\Delta A)^{-1}$ vs time, is shown in Figure 4c. Examinations of the plots suggest that the data are better fit in terms of a second-order rate law.

The other CO-loss species, observed using IR spectroscopy following flash photolysis of $\text{Cp}_2\text{Fe}_2(\text{CO})_4$ under Ar and assigned to $\text{Cp}_2\text{Fe}_2(\mu\text{-CO})_2(\mu\text{-}\eta^1, \eta^2\text{-CO})$, disappears over 2–3 h. Although $\text{Cp}_2\text{Fe}_2(\mu\text{-CO})_2(\mu\text{-}\eta^1, \eta^2\text{-CO})$ is considerably more stable under Ar than $\text{Cp}_2\text{Fe}_2(\mu\text{-CO})_3$, it is formed in much smaller amounts.^{8a,9} Thus the initial concentrations of $\text{Cp}_2\text{Fe}_2(\mu\text{-CO})_3$ and CO are close to being equal, and second-order kinetics should be observed for disappearance of $\text{Cp}_2\text{Fe}_2(\mu\text{-CO})_3$, assuming that the secondary photolysis due to the probe beam is not important in our experiment.

(B) Flash Photolysis in the Presence of CO. Flash photolysis of $\text{Cp}_2\text{Fe}_2(\text{CO})_4$ in hexane was also carried out

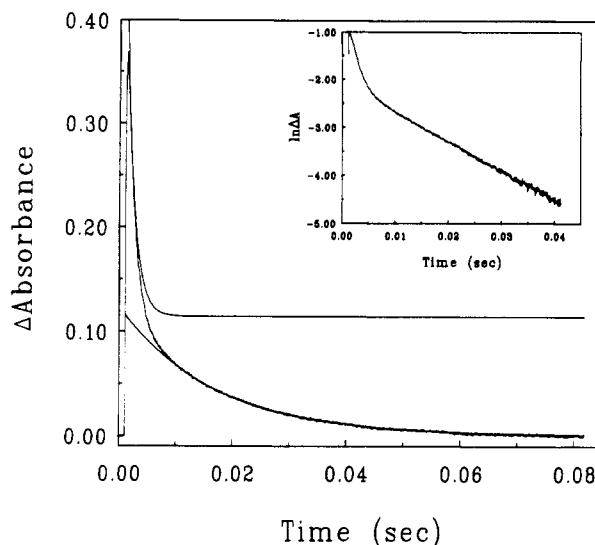
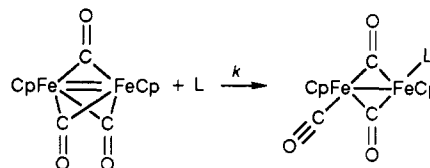


Figure 5. Plot of Δ absorbance vs time, monitored at 510 nm following flash photolysis of $\text{Cp}_2\text{Fe}_2(\text{CO})_4$ in hexane under 1 atm of CO at 25.0 °C. The data are fitted with a sum of two exponential functions. Inset: the plot of $\ln(\Delta A)$ vs time.

Scheme II

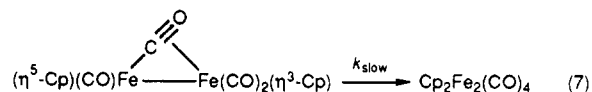


under 1 atm of CO and various CO/Ar gas mixtures. Figure 5 shows a plot of Δ absorbance vs time, monitored at 510 nm, following a flash under 1 atm of CO. The data are in excellent agreement with two first-order processes as shown in Figure 5 by the fits using two-exponential functions and the plot of $\ln(\Delta A)$ vs time shown in the inset. By varying the concentration of CO¹⁷ in solution by using CO/Ar cover gas mixtures, it was found that the observed rate constant for the fast process increases linearly with [CO] (eq 6, vide infra), whereas the rate constant

$$k_{\text{fast}} = k[\text{CO}] \quad (6)$$

$$k = (5.67 \pm 0.09) \times 10^4 \text{ M}^{-1} \text{ s}^{-1}$$

for the slow process is independent of [CO], $k_{\text{slow(av)}} = 62.4 \pm 1.5 \text{ s}^{-1}$. The observed fast and slow processes have been attributed to reactions of $\text{Cp}_2\text{Fe}_2(\mu\text{-CO})_3$, eq 5, and a new intermediate, assigned to $(\eta^5\text{-Cp})(\text{CO})\text{Fe}(\mu\text{-}\eta^1, \eta^2\text{-CO})\text{Fe}(\text{CO})_2(\eta^3\text{-Cp})$ (eq 7), respectively.^{8a,9} The new species has



been identified using time-resolved UV-vis spectroscopy and low-temperature IR spectroscopy and is reported on elsewhere.⁹ The rate constant for disappearance of $\text{Cp}_2\text{Fe}_2(\mu\text{-CO})_3$ measured by Caspar and Meyer in cyclohexane under 1 atm of CO, 280 s^{-1} ,^{2a} is lower than the values of 550 s^{-1} observed by Turner and co-workers in cyclohexane,^{4a} using time-resolved IR spectroscopy, and that observed in our experiments in hexane, 750 s^{-1} . The discrepancy may be due to the existence of the process in eq 7 which could have affected the value estimated for the

(17) *Carbon Monoxide*; Cargill, R. W., Ed.; Solubility Data Series; Pergamon Press: New York, 1990; pp 51–52.

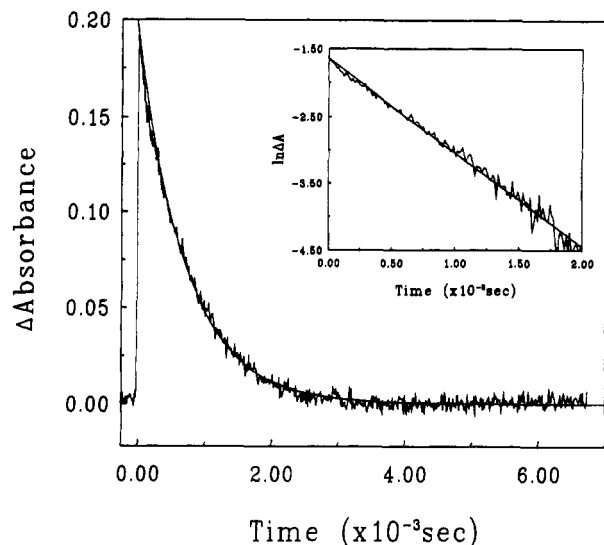
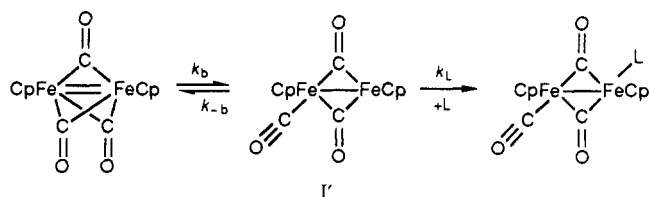


Figure 6. Plot of Δ absorbance vs time, monitored at 510 nm following laser flash photolysis of $\text{Cp}_2\text{Fe}_2(\text{CO})_4 + \text{CH}_3\text{CN}$ in hexane at 25.0 °C. The data are fitted with an exponential function. Inset: the plot of $\ln(\Delta A)$ vs time.

Scheme III



$$k_{\text{obsd}} = \frac{k_b k_L [\text{L}]}{k_{-b} + k_L [\text{L}]} \quad (8)$$

$$k_{\text{obsd}} = (k_b k_L / k_{-b}) [\text{L}] \quad (9)$$

rate constant in Caspar and Meyer's experiments.

(C) Flash Photolysis in the Presence of CH_3CN . The reactions of $\text{Cp}_2\text{Fe}_2(\mu\text{-CO})_3$ with nucleophiles (L) have been suggested to occur by an associative bimolecular pathway (Scheme II). The rate law is $k_{\text{obsd}} = k[\text{L}]$, where k_{obsd} is the pseudo-first-order rate constant. It is also possible, however, that the reactions take place via a non-associative pathway involving an intramolecular bridge-cleavage step (Scheme III). Assuming a steady-state concentration of I', the appropriate rate law expression is eq 8. If the bridge-reformation step (k_{-b}) is very fast compared to the trapping of I' by L, $k_{-b} \gg k_L[\text{L}]$, the rate law simplifies to a simple first-order dependence on [L], eq 9. However, if $k_L[\text{L}]$ is comparable in magnitude with k_{-b} , the reaction rate law will deviate from eq 9. To test the possibility that the rate law could follow eq 8, we have employed CH_3CN as a test ligand. It affords a clean reaction (eq 10) with good signal-to-noise ratio in flash photolysis measurements.

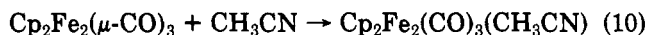


Figure 6 shows the signal obtained by using laser (308 nm) flash photolysis. The exponential fit to the data and the linear $\ln(\Delta A)$ vs time plot (inset) are consistent with a pseudo-first-order rate law. It was noted that multiple flashes using either xenon lamps or the excimer laser do not alter the pseudo-first-order rate constant for a given solution. The absorbance change following the second flash is usually greater than that following the first flash. Since considerable conversion of $\text{Cp}_2\text{Fe}_2(\text{CO})_4$ to $\text{Cp}_2\text{Fe}_2(\text{CO})_3(\text{CH}_3\text{CN})$ (Figure 1) was observed after a single flash,

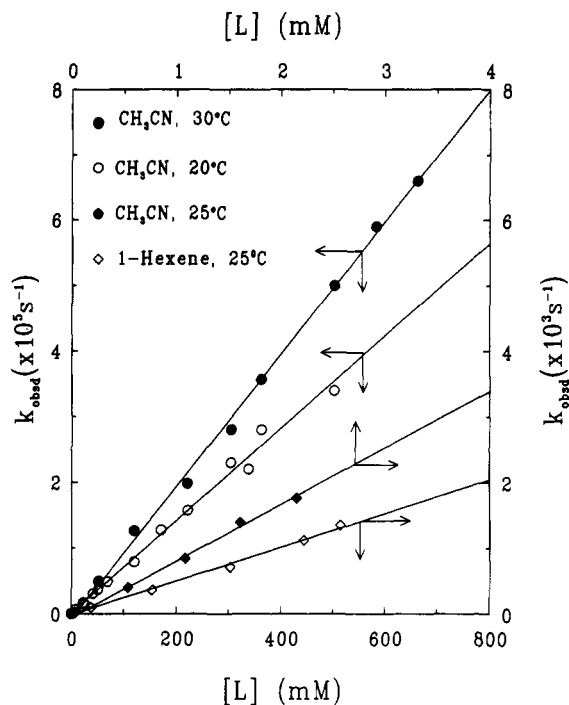
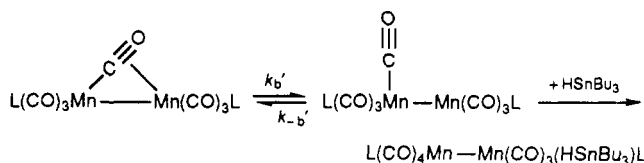


Figure 7. Plots of k_{obsd} vs $[\text{CH}_3\text{CN}]$ for data at three temperatures and a plot of k_{obsd} vs [1-hexene] for reactions with 1-hexene at 25.0 °C.

Scheme IV



the phenomenon indicates that photolysis of $\text{Cp}_2\text{Fe}_2(\text{CO})_3(\text{CH}_3\text{CN})$ also generates $\text{Cp}_2\text{Fe}_2(\mu\text{-CO})_3$ via loss of CH_3CN , and that the quantum yield of this process is greater than for loss of CO from $\text{Cp}_2\text{Fe}_2(\text{CO})_4$.

The concentration of CH_3CN was varied from 0.36 mM to the solubility maximum of 502 mM for flash photolysis at 20 °C. At 30 °C, the solubility limit is about 660 mM. Plots of k_{obsd} vs $[\text{CH}_3\text{CN}]$ at three temperatures are shown in Figure 7. The results suggest that the reaction rate law strictly obeys eq 9 over the entire concentration range. If Scheme III is a correct description of the reaction mechanism, then $k_{-b} \gg k_L[\text{CH}_3\text{CN}]$ at 30 °C, even when $[\text{CH}_3\text{CN}] = 0.66 \text{ M}$. Thus, $k_b \gg 6.6 \times 10^5 \text{ s}^{-1}$. This value is at least 10^3 times greater than the rate constant of the bridge-cleavage process (k_b'), estimated for the analogous process in dinuclear manganese carbonyls, Scheme IV.¹¹

(D) Reactions of $\text{Cp}_2\text{Fe}_2(\mu\text{-CO})_3$ with Various Nucleophiles. Conventional flash photolysis studies at 25.0 ± 0.2 °C of the reactions of $\text{Cp}_2\text{Fe}_2(\mu\text{-CO})_3$ with nucleophiles were carried out for a variety of ligands. A plot of k_{obsd} vs [1-hexene] is shown in Figure 7. Similar plots for other ligands (Figure 8) yielded linear relationships between k_{obsd} and [L]. The second-order rate constants calculated from slopes of the plots are listed in Table II. The rate constants for reactions with HSiEt_3 and H_2O were found to be too small to measure. Turner and co-workers also reported the lack of reactivity between $\text{Cp}_2\text{Fe}_2(\mu\text{-CO})_3$ and $\text{P}(o\text{-tolyl})_3$ or THF. We have reexamined the reaction of $\text{Cp}_2\text{Fe}_2(\mu\text{-CO})_3$ with $\text{P}(o\text{-tolyl})_3$ and found that the rate constant is measurable. However, non-pseudo-first-order kinetics was observed when $[\text{P}(o\text{-tolyl})_3] < 20 \text{ mM}$ due to

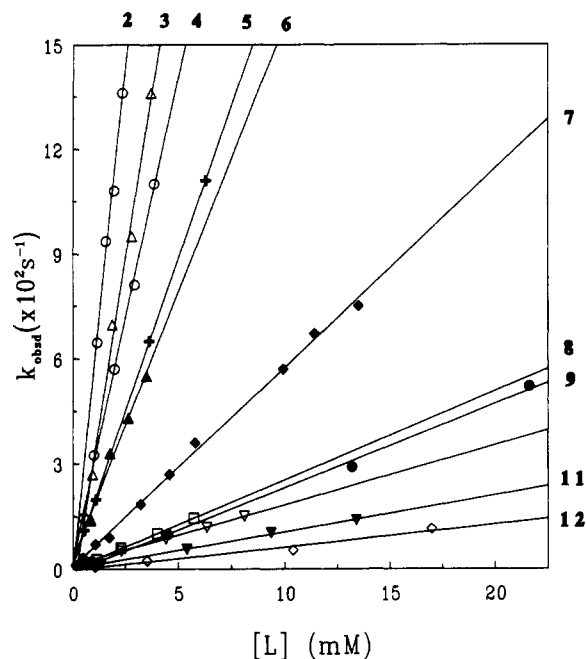


Figure 8. Plots of k_{obsd} vs $[L]$ for various ligands at 25.0 °C.

Table II. Rate Constants for Reactions of $\text{Cp}_2\text{Fe}_2(\mu\text{-CO})_3$ with Various Ligands in Hexane at 25 °C and the Electronic and Steric Parameters^a for Some Ligands

ligand	$10^{-4}k$ ($\text{M}^{-1} \text{s}^{-1}$) ^b	δ	θ	E_R	
1	CH_3CN	86 ± 4	(2.69)	(95)	(7)
2	$\text{P}(\text{OMe})_3$	58 ± 4	3.18	107	52
3	$\text{P}(\text{O-}i\text{-Pr})_3$	38 ± 2	3.90	130	74
4	PPh_3	28 ± 1	4.30	145	75
5	PBu_3	17.5 ± 0.1	5.69	132	64
6	$\text{P}(\text{OPh})_3$	15 ± 1	1.69	128	65
7	CO	5.67 ± 0.09	0	95	7
8	$\text{PPh}_2(\text{C}_6\text{F}_5)$	2.54 ± 0.04	3.13	158	79
9	$\text{P}(i\text{-Pr})_3$	2.4 ± 0.1	6.20	160	109
10	PCy_3	1.71 ± 0.01	6.32	170	116
11	$\text{PPh}(\text{C}_6\text{F}_5)_2$	0.76 ± 0.03	(1.84)	(171)	92
12	$\text{P}(t\text{-Bu})_3$	0.65 ± 0.06	6.37	182	154
13	$\text{P}(o\text{-Tolyl})_3$	~ 0.008	3.67	194	113
14	$\text{P}(\text{C}_6\text{F}_5)_3$	~ 0.002	(0.56)	184	104
15	HSnBu_3^c	12.6 ± 0.4			
16	$\text{H}_2\text{C}=\text{CHBu}$	0.257 ± 0.006			
17	$\text{HC}=\text{CBu}^d$	12.5 ± 1.2			

^a Values in parentheses are estimated. ^b Errors are 1 standard deviation. ^c Reference 8b. ^d $k = (6.24 \pm 0.59) \times 10^4 \text{ M}^{-1} \text{ s}^{-1}$ (in toluene)^{7b} has been determined, it was estimated $k(\text{in hexane}) \approx 2 k(\text{in toluene})$ by comparisons of data available in the literature.^{4c,7b,c}

the CO recombination reaction (Figure 4). The reaction with $\text{P}(\text{C}_6\text{F}_5)_3$ is also very slow; the rate constant could only be estimated (Table II). The rate constants for the studied ligands vary over 4 orders of magnitude. These results indicate that both steric and electronic properties of the

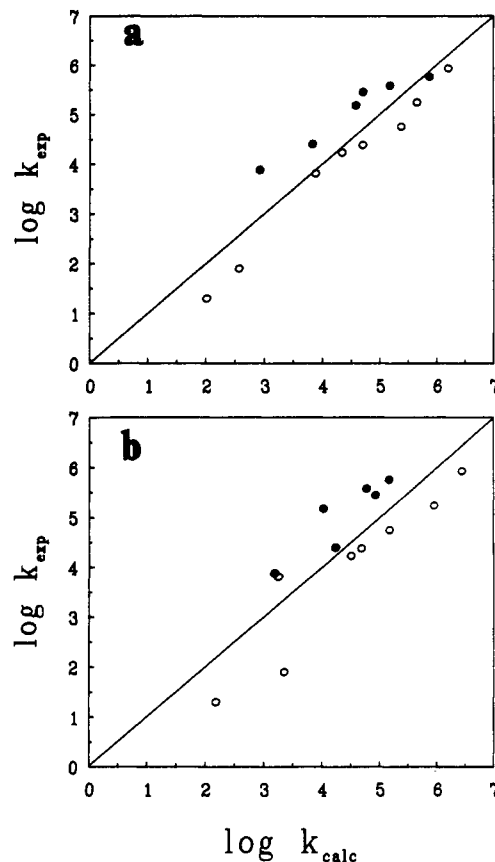


Figure 9. Plots of $\log k_{\text{exp}}$ vs $\log k_{\text{calc}}$ for 14 ligands. Ligands 1, 5, 7, 9, 10, and 12–14 are represented by open circles, whereas ligands 2–4, 6, and 8 are represented by closed circles: (a) for $S = \theta$; (b) for $S = E_R$.

nucleophiles affect their reactivities toward $\text{Cp}_2\text{Fe}_2(\mu\text{-CO})_3$.

We have also determined the activation parameters for reactions of $\text{Cp}_2\text{Fe}_2(\mu\text{-CO})_3$ with CH_3CN , CO and 1-hexene, which extend the data reported by others (Table III). The entropies of activation vary from -11 to -21 eu, suggesting that the steric character of the ligand is important in affecting the rate. The relatively higher ΔH^\ddagger for CO is consistent with a transition state in which $\text{Fe}(\mu\text{-CO})\text{Fe}$ bond breaking is relatively more advanced than $\text{Fe}-\text{CO}$ bond formation. The extreme case for such a pathway is described in Scheme III. The ΔH^\ddagger values for PPh_3 and $\text{MeOCC}\equiv\text{CCOOMe}$ are relatively smaller than expected, possibly because of interactions of the metal center with the phenyl ring on PPh_3 or the oxygen moieties on $\text{MeOCC}\equiv\text{CCOOMe}$ (vide infra).

To gain further insights into the mechanism of reactions of $\text{Cp}_2\text{Fe}_2(\mu\text{-CO})_3$ with nucleophiles, we have analyzed the kinetics data in terms of linear-free-energy relationships. Bodner's δ value based on the ^{13}C NMR chemical shifts of CO in $\text{LNi}(\text{CO})_3$ complexes,¹⁸ is used as the ligand

Table III. Activation Parameters for Reactions of $\text{Cp}_2\text{Fe}_2(\mu\text{-CO})_3$

ligand	$10^{-4}k$ ($\text{M}^{-1} \text{ s}^{-1}$, 25 °C)	ΔH^\ddagger (kcal mol ⁻¹)	ΔS^\ddagger (eu)	solvent	ref
$\text{H}_2\text{C}=\text{CHBu}$	0.26	7.2 ± 0.06	-18.5 ± 0.2	hexane	a
CO	5.67	7.6 ± 0.2	-11.5 ± 0.8	hexane	a
CH_3CN	86	5.9 ± 0.1	-11.7 ± 0.9	hexane	a
CH_3CN	76	5.8	-12.0	cyclohexane	4c
PBu_3	12.5	6.7	-12.5	cyclohexane	4c
PPh_3	21	5.3	-15.5	cyclohexane	4c
$\text{HC}=\text{CBu}$	6.2	6.2 ± 0.2	-16.6 ± 0.6	toluene	7b
$\text{HC}=\text{CPh}$	3.6	6.8 ± 0.3	-14.8 ± 0.8	toluene	7b
$\text{MeOCC}\equiv\text{CCOOMe}$	3.2	5.0 ± 0.4	-21.2 ± 1.0	toluene	7b

^a This work.

Table IV. Results of Linear-Free-Energy Analysis Using Eq 11

ligands	S	R	10a	10 ² b	c	set
1-14	θ	0.915	3.08	-3.97	9.14	1
1-14	E_R	0.836	4.72	-3.35	5.41	2
1, 5, 7, 9, 10, 12-14	θ	0.996	3.92	-4.18	8.74	3
2-4, 6, 8, 11	θ	0.974	2.75	-2.61	7.87	4
1, 5, 7, 9, 10, 12-14	E_R	0.945	5.69	-3.39	4.56	5
2-4, 6, 8, 11	E_R	0.931	3.16	-4.11	7.08	6

electronic parameter; Tolman's cone angle, θ ,¹⁹ or the ligand repulsive energy, E_R ,²⁰ is employed as the steric parameter (Table II). We employed a three-parameter multivariate regression for the linear-free-energy correlation of the kinetics data, eq 11, where $S = \theta$ or E_R . The results are summarized in Table IV.

$$\log k_{\text{calc}} = a\delta + bS + c \quad (11)$$

The correlations for the 14 ligands (Table II; sets 1 and 2 in Table IV) are shown in Figure 9 with plots of $\log k_{\text{exp}}$ vs $\log k_{\text{calc}}$. The correlation coefficients are 0.915 and 0.836 for $S = \theta$ and E_R , respectively. In both correlations the variation in steric parameter among the ligands studied accounts for 60–70% of the predicted range of rate constant values. In Figure 9, PPh_3 , $\text{PPh}(\text{C}_6\text{F}_5)_2$, $\text{PPh}_2(\text{C}_6\text{F}_5)$, and phosphite ligands are different (closed circles) from the remaining ligands (open circles). It can be seen that PPh_3 , $\text{PPh}(\text{C}_6\text{F}_5)_2$, $\text{PPh}_2(\text{C}_6\text{F}_5)$, and two of the phosphites react with $\text{Cp}_2\text{Fe}_2(\mu\text{-CO})_3$ more rapidly than predicted by the linear regression for $S = \theta$. When the two groups of ligands are subjected to regression analysis separately, the correlation coefficients for both correlations are improved (Table IV). Figure 10a,b show the plots of $\log k_{\text{exp}}$ vs $\log k_{\text{calc}}$ for $S = \theta$ and E_R , respectively, where $\log k_{\text{calc}}$ is calculated using coefficients (a, b, and c) listed in sets 3 and 5 of Table IV, respectively.

It appears that for those ligands containing an unsubstituted phenyl ring or oxygen atom, there is a consistent enhancement in rate over that predicted from the values of δ and θ or E_R for the ligands. This effect, which has not heretofore been noted as a systematic effect, could arise because the steric or electronic parameters for these ligands are systematically displaced from those for the other ligands studied. Alternatively, the enhanced rates could arise because the phenyl ring or an oxygen lone pair of the ligand interacts with $\text{Cp}_2\text{Fe}_2(\text{CO})_3$ and in doing so lowers the barrier to reaction. The magnitude of the rate enhancement is as high as 40-fold, which correspond to about 1–2 kcal mol⁻¹ in the free energy of activation. In this connection, it is significant that the ΔH^\ddagger values are lowest for PPh_3 and $\text{MeOCC}\equiv\text{CCO}Me$. The latter ligand could interact with the metal center through the lone pairs of the carbonyl oxygens.

The hypothesized interaction between ligand and metal complex would not be very strong energetically. It could

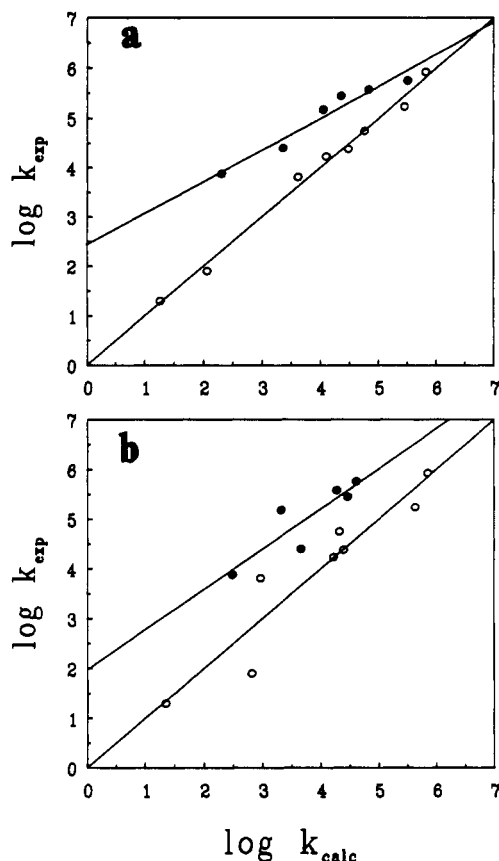


Figure 10. Plots of $\log k_{\text{exp}}$ vs $\log k_{\text{calc}}$. Ligands 1, 5, 7, 9, 10, and 12–14 are represented by open circles, whereas ligands 2–4, 6, and 8 are represented by closed circles. (a) For $S = \theta$, $\log k_{\text{calc}}$ is calculated using coefficients listed in set 3 of Table IV. (b) For $S = E_R$, $\log k_{\text{calc}}$ is calculated using coefficients listed in set 5 of Table IV.

be argued that the effect noted can best be accounted for in terms of the open form, I' of Scheme III, since this would be the least sterically hindered and most electrophilic of the various plausible reaction forms of $\text{Cp}_2\text{Fe}_2(\text{CO})_3$.

In summary, the kinetics studies reveal that the reactions of $\text{Cp}_2\text{Fe}_2(\text{CO})_3$ with a wide range of nucleophiles all obey a simple second-order rate law. The rate constants, extending over 4 orders of magnitude, depend on both the electron donor character and steric requirement of the ligand. The low enthalpies of activation for the substitution reactions, point to a low barrier to opening of the bridging structure, either in a preequilibrium step preceding ligand binding or via a concerted associative displacement.

Acknowledgment. This research was supported by the National Science Foundation through Grant CHE89-12773.

Supplementary Material Available: Tables of pseudo-first-order rate constants for reactions of $\text{Cp}_2\text{Fe}_2(\mu\text{-CO})_3$ with various ligands (6 pages). Ordering information is given on any current masthead page.

OM920319V

(18) Bodner, G. M.; May, M. P.; McKinney, L. E. *Inorg. Chem.* 1980, 19, 1951.

(19) Tolman, C. A. *Chem. Rev.* 1977, 77, 313.

(20) (a) Caffery, M. L.; Brown, T. L. *Inorg. Chem.* 1991, 30, 3907. (b) Lee, K. J.; Brown, T. L. *Inorg. Chem.* 1992, 31, 289. (c) Brown, T. L. *Inorg. Chem.* 1992, 31, 1286.